ACS APPLIED MATERIALS & INTERFACES

Forum Article

www.acsami.org

Methacrylate Copolymers with Liquid Crystalline Side Chains for Organic Gate Dielectric Applications

Andreas Berndt,*[,†,‡,§] Doris Pospiech,*[,‡,§] Dieter Jehnichen,[‡] Liane Häußler,[‡] Brigitte Voit,[†,‡,§] Mahmoud Al-Hussein,[∥] Matthias Plötner,[§,⊥] Amit Kumar,[§,⊥] and Wolf-Joachim Fischer[§,⊥]

[†]Organic Chemistry of Polymers, Technische Universität Dresden, 01069 Dresden, Germany

[‡]Leibniz-Institut für Polymerforschung Dresden e.V., Hohe Straße 6, 01069 Dresden, Germany

[§]Center for Advancing Electronics Dresden (cfaed), Technische Universität Dresden, 01062 Dresden, Germany

[∥]Physics Department, The University of Jordan, Amman 11942, Jordan

[⊥]Institute of Semiconductors and Microsystems, Microsystems Technology, Technische Universität Dresden, 01069 Dresden, Germany

Supporting Information

ABSTRACT: Polymers for all-organic field-effect transistors are under development to cope with the increasing demand for novel materials for organic electronics. Besides the semiconductor, the dielectric layer determines the efficiency of the final device. Poly(methyl methacrylate) (PMMA) is a frequently used dielectric. In this work, the chemical structure of this material was stepwise altered by incorporation of cross-linkable and/or self-organizing comonomers to improve the chemical stability and the dielectric properties. Different types of cross-linking methods were used to prevent dissolution, swelling or intermixing of the dielectric e.g. during formation processes of top electrodes or semiconducting layers. Self-organizing comonomers were expected to influence the dielectric/semiconductor interface, and moreover, to enhance the chemical resistance of the dielectric. Random copolymers were obtained by free radical and reversible addition−fragmentation chain transfer (RAFT) polymerization. With 6-[4-(4′-cyanophenyl)phenoxy]alkyl side chains having hexyl or octyl spacer, thermotropic liquid crystalline (LC) behavior and nanophase separation into smectic layers was observed, while copolymerization with methyl methacrylate induced molecular disorder. In addition to chemical, thermal and structural properties, electrical characteristics like breakdown field strength (E_{BD}) and relative permittivity (k) were determined. The dielectric films were studied in metal−insulator−metal setups. E_{BD} appeared to be strongly dependent on the type of electrode used and especially the ink formulation. Cross-linking of PMMA yielded an increase in E_{BD} up to 4.0 MV/cm with Ag and 5.7 MV/cm with PEDOT:PSS electrodes because of the increased solvent resistance. The LC side chains reduce the ability for cross-linking resulting in decreased breakdown field strengths.

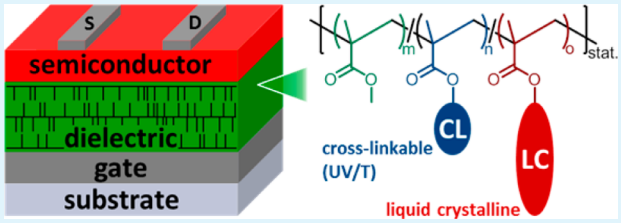

KEYWORDS: *methacrylate copolymers, liquid crystalline side chain polymers, dielectric layer, breakdown field strength, relative permittivity*

INTRODUCTION

Traditional microelectronics is based on inorganic materials such as silicon and silicon dioxide. These materials have limitations with respect to processability and flexibility. Polymeric materials can outweigh these drawbacks. Processability from melt or solution, high flexibility of films, light weight, and printability are reasons for a continuous and strong increase of interest in all-organic electronics. These properties open up the way to large scale applications in cost-efficient processes.[1] Moreover, the characteristics of polymers can be widely designed by their basic chemical structure. A variety of research results in the field of organic electronics has been reported so far[2−4] but only a few are presently used in practice. Possible applications for organic materials in electronic devices are organic light-emitting diodes (OLEDs),[5] organic field-effect transistors (OFETs),[6−8] organic photovoltaics (OPVs),[9] sensors,[10] lasers,[11] radio frequency identification (RFID) tags,[12] and more. Requirements that polymers and organic materials in general should meet for these applications are a good availability, the opportunity of using solution-based deposition processes at low temperature and low-cost production in high throughput.[1,13]

In 1990, the first working OFETs with polymeric gate dielectrics were fabricated by Peng et al.[14] Cyanoethylpullulan (CYPEL), poly(vinyl alcohol) (PVA), poly(vinyl chloride) (PVC), poly(methyl methacrylate) (PMMA), and poly(styrene)

Special Issue: Forum on Polymeric Nanostructures: Recent Advances toward Applications

Received: October 9, 2014
Accepted: November 25, 2014
Published: December 12, 2014

 © 2014 American Chemical Society dx.doi.org/10.1021/am5069479 | ACS Appl. Mater. Interfaces 2015, 7, 12339−12347

(PS), respectively, were applied as dielectric layers. Also in that year, the first working all-organic transistor with CYPEL as organic gate dielectric was fabricated by the same group.[15] Since then, a lot of research focused on optimized materials for organic gate insulators.[13,16,17]

The aim of this work is to provide new dielectric materials with an increased relative permittivity based on methacrylate chemistry. The reason for the development of high-k materials originates from the need for strong field coupling across the OFETs gate insulator described by eqs 1 and 2[13,18]

$$C_i = \frac{\varepsilon_0 k}{d} \quad (1)$$

$$(I_{SD})_{sat} = \frac{W}{2L}\mu C_i (V_{SG} - V_T)^2 \quad (2)$$

where C_i is the capacitance of the dielectric per unit area, ε_0 the permittivity of free space, k the relative permittivity, d the thickness of the dielectric layer, $(I_{SD})_{sat}$ the drain current in saturation regime, W the channel width, L the channel length, μ the charge carrier mobility, V_{SG} the gate voltage and V_T the threshold voltage. Raising permittivity k of the dielectric layer will allow higher film thicknesses resulting in lower gate leakage without decrease of capacitance C_i. Higher capacitances C_i at the same thickness allow lower operating voltages and thus lower power consumption, which is an important aspect of transistor technology.

PMMA is often applied as organic dielectric[19−24] and therefore, it was reasonable to take it as base structure for copolymers. The aim was to use the advantages of PMMA and to further optimize this material by introducing comonomers with specific properties. This is a straightforward approach to new dielectrics with tailored characteristics. The relative permittivity of PMMA is 3.2−3.6.[25,26] Other polymeric dielectrics like polyvinylphenol, PVA or CYPEL have higher permittivities of 4.2−5,[27,28] 7.8−10,[14,28] or 12−18.5,[14,15,28] respectively. However, these polymers contain OH-groups that can act as charge traps at the dielectric/semiconductor interface, which should be avoided.

The polymer system investigated in this work includes methyl methacrylate (MMA), cross-linkable methacrylates, and liquid crystalline (LC) side chain comonomers to induce self-organization in the system.

Growth, packing and crystallinity of an organic semiconductor are strongly influenced by the substrate.[29] The effect of the substrate is mainly transferred by the dielectric/semiconductor interface. Thus, the structure and composition of the dielectric plays a vital role. Self-organization of the dielectric material is expected to result in the formation of a well ordered dielectric thin film. The effect of ordered dielectric layers on the morphology of the semiconductor and the performance and charge carrier mobility of devices has already been shown for dielectric self-assembled monolayers (SAMs). Several research groups published higher charge carrier mobilities for higher-ordered octadecylsilane-modified (OTS) SiO_2 dielectric layers. For pentacene, Lee et al.[30] reported a mobility of about 0.6 $cm^2 V^{-1} s^{-1}$ for dense OTS compared to 0.3 $cm^2 V^{-1} s^{-1}$ for less-ordered OTS layers. Lin et al.[31] noted charge carrier mobilities of 2.0 and 0.6 $cm^2 V^{-1} s^{-1}$, respectively. For C_{60}, the effect was even higher than for pentacene. The mobility increased to 4.5 $cm^2 V^{-1} s^{-1}$ when fabricated on crystalline OTS instead of 0.2 $cm^2 V^{-1} s^{-1}$ on the lowest ordered OTS.[31] Many different small molecule organic semiconductors were investigated with respect to this matter.[32,33] In all cases, the mobilities were higher when deposited on ordered OTS layers. From these results the importance of the dielectric/semiconductor interface becomes obvious and thus the chemistry and order of the dielectric itself.

With respect to processability and large scale applications, SAMs exhibit some limitations. To overcome these weaknesses, ordered dielectric polymers are promising. If suitable LC comonomers are incorporated in PMMA, nanophase separation could be achieved resulting in layered nanostructures with ordered and densely packed side chains. This has been shown for methacrylate copolymers with semifluorinated side chains.[34] Similar effects as observed for highly ordered SAMs can be expected for LC copolymers to create a dielectric/semiconductor interface with defined chemistry and order resulting in enhanced semiconductor morphology, higher charge carrier mobilities and better performances of OFETs. Before the applicability of LC copolymers as dielectrics in OFETs can be characterized, their solution processability, cross-linkability, self-assembling behavior and dielectric properties such as breakdown field strength and relative permittivity have to be thoroughly studied. Results of this work are discussed here. OFET fabrication and characterization are presently investigated and will be published in near future, also including gate leakage, hysteresis, and other electrical characteristics.

An additional effect expected after introduction of LC comonomers is reduced solubility in common solvents compared to PMMA. This, in turn, causes improved solvent resistance which is important when the semiconductor layer is processed on the dielectric in device fabrication from solution. On the other hand, a certain solubility of the dielectric has to be assured in order to guarantee solution processing.

Furthermore, the used liquid crystalline methacrylate comonomers contain polar terminal cyano groups to influence the relative permittivity.

Different types of cross-linkers (CL) were employed to further improve both mechanical and solvent stability. From cross-linking, several positive effects are assumed to occur. First of all, cross-linking prevents the dielectric layer from dissolving, swelling and intermixing with neighboring layers. This is important for the solution fabrication of multilayer devices where, for example, the semiconductor is placed on top of the dielectric (bottom gate transistors). Additionally, the inks presently used to print the electrodes, e.g., silver inks, contain at least partially organic solvents which are able to swell or damage the dielectric layer. Moreover, cross-linking protects the dielectric film from diffusion of impurities, e.g. during inkjet printing. All these effects should finally lead to significant improvement of breakdown field strength and thus, to a better device performance.

The materials of this work are developed for organic/all-organic field-effect transistors with improved performances. One advantage of methacrylate copolymers is their solution processability. Important electrical requirements for dielectrics are high breakdown field strengths and high relative permittivities. The former is important to fabricate thinner layers to increase capacitance, to lower operating voltages and power consumption, and to enhance the switching behavior. High permittivities further increase the capacitance. So, an optimized dielectric film thickness will reduce leakage currents. To the best of our knowledge, dielectric liquid crystalline side chain copolymers were not the subject of previous OFET investigations.

Scheme 1. Synthetic Routes to LC Copolymers and Cross-linking Strategies Used

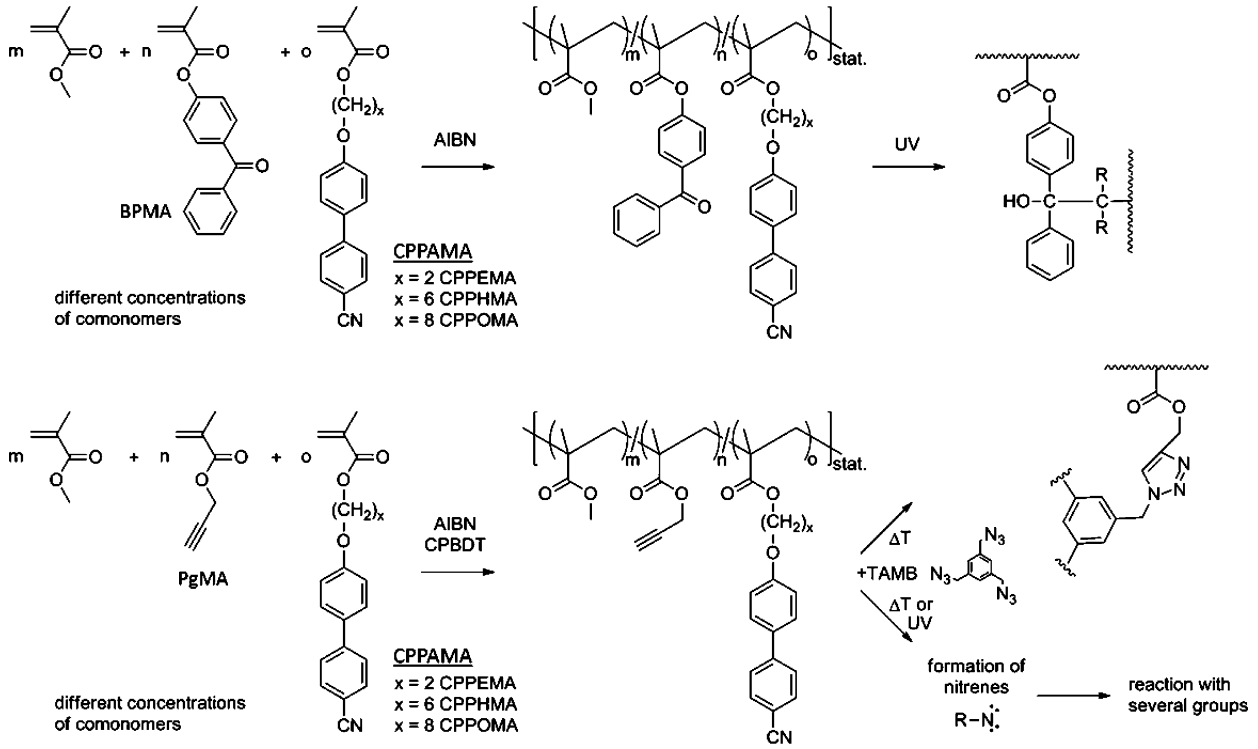

Table 1. Chemical Compositions, Molecular Weights, and Transition Temperatures of the Copolymers under Study

no.	polymer	comp. [mol %]	M_n [kg/mol]	M_w [kg/mol]	M_w/M_n	T_g [°C]	T_i [°C]
1	PMMA	100	41.6	73.7	1.77	127	
2	P(MMA/BPMA)	91/9	59.4	126.9	2.14	128	
3	P(MMA/PgMA)[a]	89/11	62.9	294.7	4.69	122	
4	P(CPPEMA) (x = 2)	100	42.4	149.4	3.52	121	
5	P(MMA/CPPEMA)	47/53	42.3	113.3	2.68	121	
6	P(MMA/BPMA/CPPEMA)	35/11/54	50.9	129.7	2.55	122	
7	P(MMA/PgMA/CPPEMA)[a]	35/13/52	52.1	420.8	8.08	119	
8	P(CPPHMA) (x = 6)	100	100.8	259.5	2.57	62	115
9	P(MMA/CPPHMA)	49/51	46.0	94.0	2.04	68	
10	P(MMA/BPMA/CPPHMA)	38/12/50	43.4	101.2	2.33	75	
11	P(MMA/PgMA/CPPHMA)[a]	37/9/54	43.4	64.2	1.48	72	
12	P(CPPOMA) (x = 8)	100	36.3	131.0	3.61	37	119
13	P(MMA/CPPOMA)	48/52	27.1	80.6	2.97	53	
14	P(MMA/BPMA/CPPOMA)	38/11/51	30.1	100.0	3.32	59	
15	P(MMA/PgMA/CPPOMA)[a]	35/14/51	10.7	16.4	1.53	40	

[a]Synthesized by RAFT; comp.: composition determined by ^{1}H NMR; M_n: number-averaged molecular weight; M_w: weight-averaged molecular weight; M_w/M_n: polydispersity; molecular weights determined by SEC; thermal transitions determined by DSC.

The methacrylate copolymers studied were prepared by free radical solution or, if necessary, by reversible addition–fragmentation chain transfer (RAFT) polymerization without addition of any type of salts and ions because ions remaining in the dielectric layer are the main reason for low breakdown field strengths. The study presents synthesis results, physical characterization and device properties obtained for metal–insulator–metal setups (MIM) of the materials.

RESULTS AND DISCUSSION

The reaction scheme for synthesis of the different copolymers and the cross-linking strategies employed are given in Scheme 1. Copolymers of MMA with the comonomer 6-[4-(4′-cyanophenyl)phenoxy]ethyl methacrylate (CPPEMA, x = 2) or the LC comonomers 6-[4-(4′-cyanophenyl)phenoxy]hexyl methacrylate (CPPHMA, x = 6) or 6-[4-(4′-cyanophenyl)-phenoxy]octyl methacrylate (CPPOMA, x = 8), respectively, including one type of the cross-linkable monomers 4-benzoylphenyl methacrylate (BPMA) or propargyl methacrylate (PgMA) were synthesized by free radical polymerization with azobis(isobutyronitrile) (AIBN) as initiator, or by RAFT polymerization with AIBN as initiator and 2-cyano-2-propyl benzodithioate (CPBDT) as chain transfer agent, respectively. For PMMA and P(MMA/BPMA) chloroform was used as standard solvent. For the polymer series with CPPEMA and CPPOMA benzene had to be employed as solvent.[35] Copolymers with PgMA required application of RAFT polymerization with toluene as solvent.[36] For RAFT polymerizations

dx.doi.org/10.1021/am5069479 | ACS Appl. Mater. Interfaces 2015, 7, 12339–12347

with 6-[4-(4′-cyanophenyl)phenoxy]alkyl methacrylates (CPPAMA) as comonomers tetrahydrofuran (THF) or benzene were useful solvents.

The chemical composition of the random copolymers was assessed by ^{1}H NMR spectroscopy (see the Supporting Information). The copolymer composition found was close to the monomer ratio.

Table 1 summarizes the compositions of the synthesized copolymers, the molecular weights and the transition temperatures detected by differential scanning calorimetry (DSC). The number-averaged molecular weights of all samples obtained by free radical polymerization and by RAFT were between 30 and 60 kg/mol and thus in the expected range.

T_g denotes the glass transition temperature and T_i the isotropization temperature (synonymous to T_{Cl}, the clearing temperature). The homopolymer P(CPPEMA) with the 6-[4-(4′-cyanophenyl)phenoxy]ethyl side chain (spacer x = 2) showed a well-pronounced glass transition T_g but no liquid crystalline behavior as also known from literature for such a short spacer.[37−39] In contrast and also according to literature, the homopolymers P(CPPHMA) (x = 6) and P(CPPOMA) (x = 8) underwent two thermal transitions indicative for liquid crystallinity.[35,40]

Wide-angle X-ray scattering (WAXS) was carried out at room temperature to prove the existence of LC structures in the polymers under discussion (Figure 1). Comparison of P-

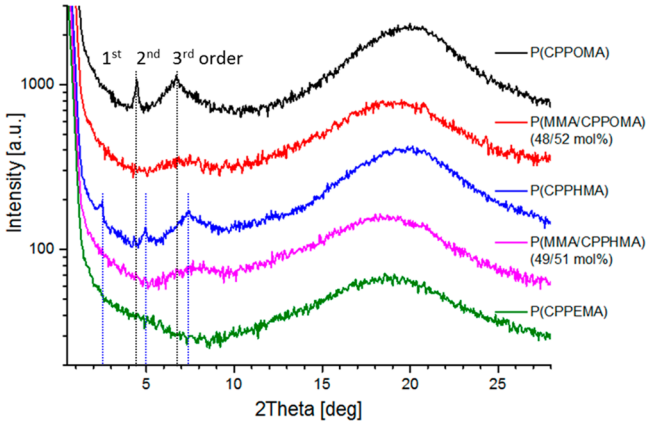

Figure 1. WAXS curves of the three homopolymers (spacer lengths x = 2, 6, 8) and the corresponding copolymers with MMA (around 50/50 mol %/mol %) at room temperature.

(CPPEMA), P(CPPHMA) and P(CPPOMA) indicated a layered structure in the latter ones (see reflections in the intermediate scattering range of 2−9° in 2θ), according to the DSC results discussed above. In these samples, thermotropic liquid crystalline phases were observed also under the polarizing microscope between T_g and T_i, and identified as smectic phases (Figure 2). The main feature of the P(CPPEMA) curve is a abroad amorphous halo at 2$\theta \approx 19°$. In contrast, the P(CPPHMA) curve exhibits three reflections at low 2θ values and a broad amorphous halo at 2$\theta \approx 20°$. The first three reflections lie at relative positions of 1:2:3 in 2θ ($\approx$ 2.46°:4.92°:7.38°) indicating the formation of a smectic phase. The smectic layer spacing calculated from the first-order reflection (2θ = 2.46°) is $d \approx 3.6$ nm, which is larger than the fully extended length of the side chain, estimated to be 2.13 nm. This indicates a partial interdigitation of the side chains in the smectic layers. A similar behavior is exhibited by the P(CPPOMA) curve

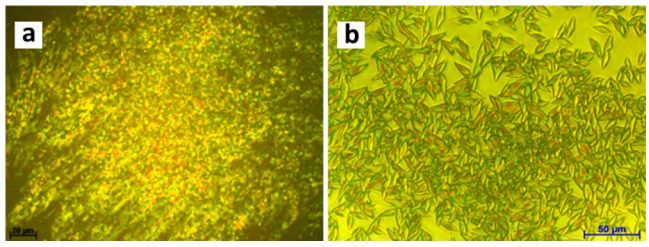

Figure 2. Thermotropic liquid crystalline phases of the homopolymers (a) P(CPPHMA) and (b) P(CPPOMA) observed by polarized microscopy on cooling from the isotropic melt at (a) 116.5 °C and (b) 121.5 °C, respectively. P(CPPHMA) showed blurred Schlieren texture, P(CPPOMA) showed Bâtonnets, which form a focal conic fan texture on further cooling (compare reference 35).

with a corresponding smectic layer spacing of ≈4.0 nm (first-order reflection has no intensity, second 4.45°, third ≈6.70°).

In the corresponding copolymers with about 50 mol % MMA a layered structure was not observed. Both homopolymers and copolymers showed a broad scattering maximum around the position of the third order reflection of the related smectic structure of the homopolymer. This maximum possessed the lowest full width at half-maximum in the case of the homopolymer. It could be concluded that because of the presence of MMA segments in the main chain the generation of a well-ordered layered structure is strongly disturbed. The interaction between the side chains is suppressed due to the presence of MMA in the main chains (dilution effect). This leads to reduced coherence lengths of the layered structure of the side chains and eventually the disappearance of the reflections of the layered structure from the scattering curve. Further discussion of the effect of increasing the MMA content on the smectic layer structure and a possible model for explaining the unusual broadness of the third order reflection will be presented in a separate work.

Thin films of these copolymers were prepared by spin coating and analyzed by ellipsometry and X-ray reflectivity (XRR). Figure 3 shows a typical X-ray reflectivity curve of a spin coated film of the homopolymer P(CPPHMA) on silicon substrate. The weakly damped single-frequency Kiessig fringes over the whole curve indicate a uniform thickness of the polymer film. To obtain more quantitative information about the film structure

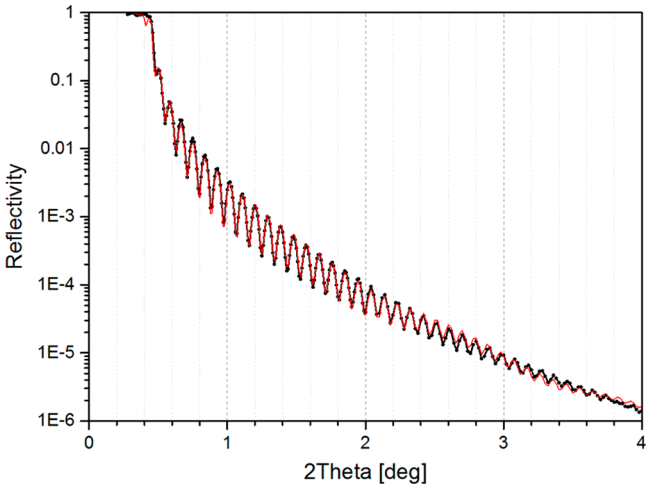

Figure 3. X-ray reflectivity curve of a P(CPPHMA) homopolymer thin film spin-coated on Si wafer. The red solid line represents the best fit.

perpendicular to the substrate, the XRR curve was fitted using different models. For each model, the sample was represented by a stack of layers; each with its own electron density, thickness, and a Gaussian interfacial roughness. The best fit of the XRR curve was achieved using a three-layer model with a total film thickness of 95 nm and low surface roughness of 3 nm. As it can be seen, the calculated reflectivity curve is in good agreement with the measured one over the investigated scattering range. It is also noticeable that Bragg reflections that could be associated with the smectic spacing of the side chains cannot be observed at small 2θ values. This implies the absence of smectic ordering along the film normal. It is conceivable that the electron density contrast between main chains and mesogenic layers is not high enough. Note that the film was not annealed in the LC temperature region in order to avoid dewetting phenomena. This situation may change if the dielectric is not the top layer as in case of bottom gate transistors. There, annealing can be used to manipulate the structure formation.

Copolymers with 50 mol % MMA show better film formation. They can be annealed without dewetting. However, they do not form ordered layers in thin films. Copolymerization leads to a distorted interlayer packing and significant reduction in the correlation size along the layer normal.[41]

Cross-linking was performed directly in spin-coated or self-supporting films using one of the strategies illustrated in Scheme 1. BPMA-containing copolymers with MMA were successfully cross-linked by UV irradiation.[42,43] In case of the copolymers with CPPAMA, the cross-linking by UV light was not as effective as for MMA/BPMA copolymers. It appears possible that the carbonyl group of BPMA which is responsible for cross-linking is shielded by the longer LC side chains. PgMA-containing copolymers were cross-linked either by thermally induced click reaction with 1,3,5-tris(azidomethyl)benzene (TAMB) yielding triazole rings,[44,45] or by photochemical and/or thermal formation of nitrenes from TAMB which can react with several groups in the polymer chain.[45−49] Also here, the presence of the CN-containing side chains in P(MMA/PgMA/CPPAMA) copolymers led to less efficient cross-linking. Films from copolymers with less efficient cross-linking were insoluble in chloroform, but not fully stable. As comparison to these cross-linking methods and to literature results, 1,6-bis(trichlorosilyl)-hexane as reported by Facchetti et al.[1,13] as well as Noh et al.[19] was added to the PMMA homopolymer. It acts as external cross-linker forming an interpenetrating network through the film without chemical linkage to the copolymer chains. After cross-linking, these films were not soluble in chloroform. However, films with higher content of this cross-linker (50 wt % with respect to PMMA) showed high roughness visible to the naked eye. Films with lower content (10 wt %) were smoother, but did not exhibit improved electrical characteristics in our measurements (see Figure 5a and 6a). The best cross-linking results in terms of solubility were found for the thermally induced reaction between PgMA-containing copolymers and TAMB (yielding triazoles combined with nitrene formation and their post reaction). These films were flexible, not colored after cross-linking, insoluble, stable and did not swell significantly in chloroform. In the next paragraph, the influence of the cross-linking method on the results of the electrical characterization will be outlined.

MIM structures were used as test setups to characterize the electrical properties of the copolymer films. A complete summary of breakdown field strengths E_{BD} and relative permittivities k calculated from breakdown voltages and capacitances measured can be found in the Supporting Information. As top electrodes, poly(3,4-ethylenedioxythiophene):polystyrenesulfonate (PEDOT:PSS) printed from a solution containing water and organic solvents and Ag electrodes printed from solution of silver neodecanoate (Ag Neo) in xylene, or a formulation of silver nanoparticles (Ag NP) in glycol ethers, respectively, were used. The main results are given in Figures 4−6. With PEDOT:PSS as

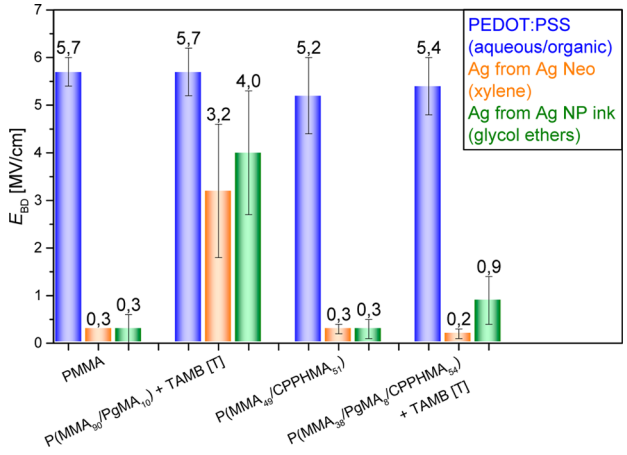

Figure 4. Breakdown field strength of cross-linked and non-cross-linked copolymers, with and without LC comonomers and with different organic and inorganic electrodes. Breakdown field strength calculated from measured breakdown voltage at a current flow of 10 nA using PEDOT:PSS or Ag from Ag Neo or Ag NP ink as electrode in MIM setup. [T]: thermally cross-linked by adding of TAMB.

electrode the breakdown field strength is not strongly influenced by the copolymer composition or by cross-linking. For all samples, E_{BD} is between 3.7 and 5.7 MV/cm (see the Supporting Information). PEDOT:PSS was printed from an aqueous solution containing parts of organic solvents. This mixture does not interact with the copolymers. Therefore, dissolving or swelling did not happen and thus, the dielectric film and its properties remained unchanged. Ag electrodes were printed from organic solvents and resulted in significant differences in the breakdown field strengths. For non-cross-linked PMMA the breakdown field strength is around 0.3 MV/cm. Here, the film was dissolved and/or swollen by the organic solvents upon printing and thus, the uniformity of the film was changed and impurities could diffuse into the layer. The value is compliant to the literature. Park et al.[20] calculated 0.3 MV/cm for atactic PMMA measured with Au electrode. After cross-linking the films, e.g., thermally with TAMB, breakdown field strength values up to 4.0 MV/cm were found indicating the increased solvent stability. These results indicate the importance of copolymerization, e.g., with cross-linkable comonomers, when compared with the low value of PMMA. Despite PEDOT:PSS yielded in very high E_{BD} also for PMMA, solution fabricated devices will use organic solvents to deposit organic semiconductors like poly(3-hexylthiophene) from chloroform on top of the organic dielectric. In that case, cross-linking, as shown in Figure 4, will be mandatory.

Xu et al.[50] reported also very high values for cross-linked polyacrylate copolymers of around 7 MV/cm with a polymer system of four different comonomers. Their cross-linking based on the reaction between carboxylic acid and epoxy groups during which the formation of OH groups occurs acting as charge traps at the dielectric/semiconductor interface. Moreover, the

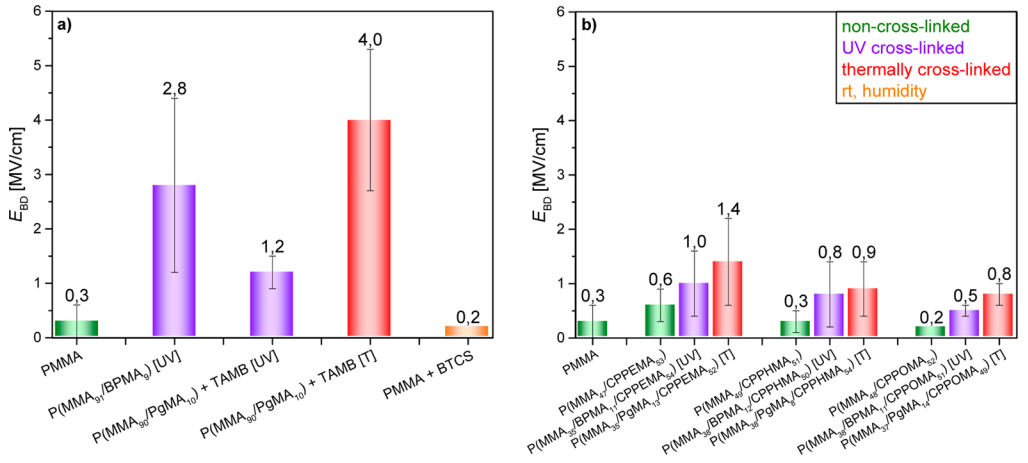

Figure 5. (a) Breakdown field strength of PMMA and cross-linked methacrylate copolymers; (b) breakdown field strength of PMMA and cross-linked copolymers containing CPPAMA comonomers. Breakdown field strength calculated from measured breakdown voltage at a current flow of 10 nA using Ag (from Ag NP ink) as electrode in MIM setup. [UV]: UV cross-linked either by BPMA or by adding of TAMB; [T]: thermally cross-linked by adding of TAMB; ext. CL, cross-linked at room temperature by adding of 1,6-bis(trichlorosilyl)hexane (external cross-linker, BTCS) because of humidity.

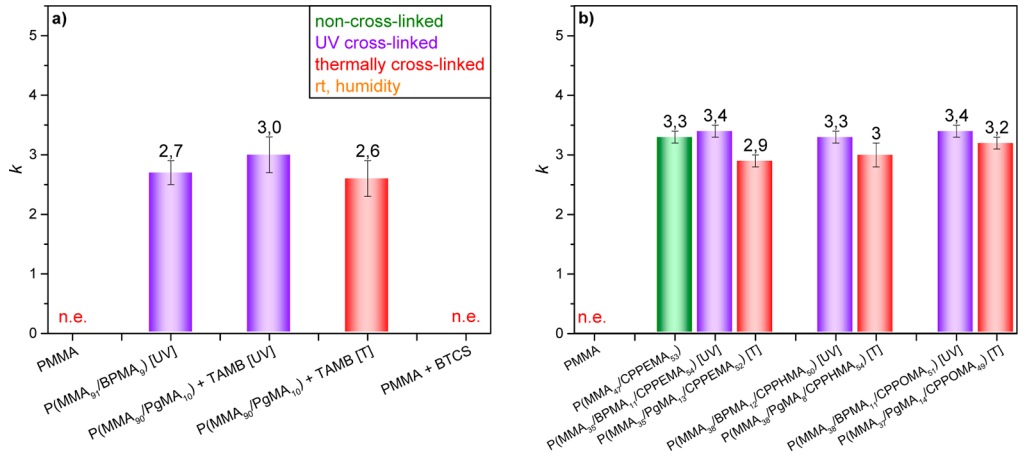

Figure 6. (a) Relative permittivity of PMMA and cross-linked methacrylate copolymers; (b) relative permittivity of PMMA and cross-linked copolymers containing CPPAMA comonomers. Relative permittivity calculated from measured capacitance at a frequency of 1 MHz using Ag (from Ag NP ink) as electrode in MIM setup. Area of printed electrodes determined by optical microscopy and film thickness by ellipsometry. [UV]: UV cross-linked either by BPMA or by adding of TAMB; [T]: thermally cross-linked by adding of TAMB; ext. CL, cross-linked at room temperature by adding of 1,6-bis(trichlorosilyl)hexane (external cross-linker, BTCS) due to humidity; n.e., not evaluable.

copolymers contain more carboxylic acid groups then necessary for the cross-linking reaction. The excess additionally remains as charge traps. High temperature (230 °C) for optimal cross-linking was required. Polyacrylate as well as polymethacrylate based copolymers are known to start degradation above 150 °C (e.g., PMMA at ≈175 °C[51]). Cross-linking reactions at such a high temperature are not well-defined. Additionally, this high temperature may not be appropriate for the handling of polymeric substrates for all-organic FETs. The present study wanted to avoid the negative influences of charge traps and high temperature.

By incorporation of LC comonomers like CPPHMA the cross-linking was partially suppressed as discussed above. This resulted in drastically reduced E_{BD}. It was also noticeable that the use of electrodes printed from xylene yielded lower values than the use of electrodes printed from glycol ethers, indicating that xylene interacts more with the copolymers. The mutual higher swelling may support the diffusion of silver salts into the polymer matrix.

Further dielectric characterization (E_{BD} and k) was done mainly with Ag electrodes printed from Ag NP ink. Reasons for that are that PEDOT:PSS is known to show limited electrical conductivity. This could yield in a changed breakdown mechanism. Additionally, measurements of capacitance were not successful with PEDOT:PSS. Better conductive materials like Ag had to be applied as top electrodes. Furthermore, dielectric properties determined with Ag electrodes are comparable with literature. Vacuum deposited metal electrodes such as Ag are often used.

Figure 5a shows that the breakdown field strength measured in a setup prepared by printing Ag NP ink which is a dispersion of NPs in a mixture of glycol ethers is increased both by UV and thermal cross-linking. The best results were observed by thermal cross-linking of P(MMA/PgMA) with TAMB. As mentioned above, this combination led to the most efficient cross-linking of the films. Using 1,3-bis(trichlorosilyl)hexane (BTCS) as external cross-linker according to Facchetti et al.[1,13] and Noh et al.[19] did not lead to an increased E_{BD} although self-supporting films were not soluble (in chloroform) after cross-linking. In case of CPPAMA-containing copolymers (Figure 5b) the suppressed cross-linking yielded significantly decreased breakdown field

dx.doi.org/10.1021/am5069479 | ACS Appl. Mater. Interfaces 2015, 7, 12339−12347

strengths. Nevertheless, there is a difference between cross-linked and non-cross-linked samples. Comparing the three different spacer lengths, CPPEMA copolymers with the ethyl spacer showed the highest E_{BD}, indicating that the spacer length and thus the developing LC character correlate with the inhibited cross-linking.

Figure 6 shows the results of the calculated relative permittivities. Because of early breakdown and/or high leakage only in case of cross-linked copolymer films evaluable capacities could be measured (except for P(MMA/CPPEMA)). The relative permittivities for cross-linked P(MMA/BPMA) and P(MMA/PgMA) lay between 2.6 to 3.0. The permittivity k found in the literature for PMMA at a frequency f of 1 MHz is 2.6.[52] The effect of the CN-containing comonomers CPPAMA on the relative permittivity k was studied. Kim et al. for example reported relative permittivities of about 12.6 to 14.1 for cyanoethylated poly(vinyl alcohol) (f = 20 Hz).[53] For methacrylate copolymers containing 50 mol % of CPPAMA comonomers the permittivities were in the range of 2.9 to 3.4. These results show a slight increase in k. With respect to the low ratio of polar CN moieties to the nonpolar parts in the CPPAMA molecules a more significant increase was not to be expected. To evaluate these results Al electrodes were deposited on PMMA and P(MMA/CPPHMA) by vapor deposition. The capacitance was measured over a frequency range and an average value of k was calculated. For PMMA k was 3.0 and for P(MMA/CPPHMA) it was 3.2. These results confirm those ones coming from printed dielectric layers.

CONCLUSIONS

In conclusion, random methacrylate copolymers with different kinds of cross-linkers and liquid crystalline side chain comonomers with different spacers were synthesized by free radical or RAFT polymerization. The results of DSC and WAXS indicated liquid crystalline behavior and the formation of smectic phases for the homopolymers of CPPHMA and CPPOMA. XRR experiments showed that smooth thin copolymer films can be originated by spin coating with reproducible film quality. Using PEDOT:PSS electrodes printed from aqueous/organic solvent mixture the breakdown field strength E_{BD} was up to 5.7 MV/cm. Here, no significant differences between cross-linked and non-cross-linked copolymer films were observed because of low solvent−copolymer interactions. In the case of silver electrodes, whose precursors were inkjet printed from organic solvents, the importance of cross-linking became obvious. With suitable cross-linking methods the breakdown field strength could be raised up to 4.0 MV/cm even with Ag electrodes e.g. printed from xylene or glycol ethers. This is a very good result for organic dielectric layers with metal electrodes both fabricated from solution. In case of CPPAMA-containing copolymers the E_{BD} values were lower due to suppressed cross-linking. The relative permittivity k of cross-linked poly(methyl methacrylate)s was around 3. By incorporation of 50 mol % of the CN-containing comonomers CPPAMA a slight increase of k could be observed. Despite of the size of these large molecules that contain the CN group, its enhancing effect on k is still present. In the case of smaller molecules or higher amount of cyano groups resulting in a higher ratio of polar CN moieties to nonpolar species, a further enhancement of k could be expected.

EXPERIMENTAL METHOD

Materials. Benzene (99.8%), 1,6-bis(trichlorosilyl)hexane (97%), butyl acetate (99.5%), ω-chloroethanol (99%), ω-chlorooctanol (98%), 2-cyano-2-propyl benzodithioate (>97%), N,N-dimethylformamid (99.8%), 4′-hydroxy-4-biphenylcarbonitril (97%), magnesium sulfate (≥98%), potassium carbonate (≥99%), sodium hydroxide (≥98%), sodium sulfate (≥99%), toluene (≥99.7%), triethylamine (≥99.5%), and 1,3,5-tris(bromomethyl)benzene (97%) were obtained from Sigma-Aldrich. Azobis(isobutyronitrile) (≥98%), chloroform (99.99%) and methacryloyl chloride (≥97%) were purchased from Fluka. ω-Chlorohexanol (97%), 4′-hydroxy-4-biphenylcarbonitril (99%) and propargyl methacrylate (98%) were obtained from Alfa Aesar. Chloroform (99.5%), ethyl acetate (99.5%), 4-hydroxybenzophenone (98%), methanol (99.99%), methylene chloride (99.99%), sodium azide (99%), sodium bicarbonate (99.5%), and tetrahydrofuran (99.99%) were purchased from Acros Organics and n-hexane (≥98.5%) and hydrochloric acid (37%) were obtained from Merck.

Methods. NMR was carried out on a Bruker DRX 500 with a frequency of 500.13 and 125.75 MHz for ^{1}H and ^{13}C, respectively, using $CDCl_3$ and CD_2Cl_2 as solvents. Size exclusion chromatography (SEC) was performed with a Knauer GPC equipped with PL MIXED-C separation column using RI detection. THF was used as eluent with a flow rate of 1.0 mL/min. Relative molar masses were calculated using calibration with narrow distributed PMMA standards. DSC curves were taken on a DSC Q1000 (TA Instruments, USA) in a temperature range from −80 to 150 °C at a heating/cooling rate of 2 K/min (modulated). Ellipsometry was carried out on a multiwavelength ellipsometer Multiscope (Optrel) and with an Alpha-SE (J. A. Woollam Co., Inc., Ellipsometry Solutions) at an angle of incidence of 65° using a CCD detector was used. Calculations were done by a 2-parameter-fit according to Cauchy[54] using the software CompleteEASE (Fa. Woollam Co. Inc.). Optical and polarized microscopy was carried out on a Axio Imager A1m (Zeiss) using AxioVision Rel. 4.8 as software. WAXS and XRR curves were recorded using a 2-circle diffractometer (XRD 3003 θ/θ, Seifert-FPM, Germany) with monochromatic Cu−Kα radiation (λ = 0.154 nm). The samples were investigated under specular reflection conditions. The electron density profile along the film normal was determined by comparing the calculated and the experimental reflectivity curves using Parratt algorithm.

Syntheses. The synthetic procedures and NMR spectra of low molecular weight compounds are provided in the Supporting Information.

General procedure for radical polymerization. The solid monomers, AIBN and, in case of RAFT polymerization, CPBDT were placed in a one-necked-flask and evacuated and nitrogen purged for three times. Then, the solvent and the liquid monomers were added. The mixture was degassed by three freeze−vacuum−thaw cycles. After that the reaction started by immersing the flask into an oil bath at the corresponding polymerization temperature. After the reaction time the mixture was diluted, precipitated the 10-fold excess of methanol, filtered, washed, and dried under reduced pressure at 50 °C. The respective ratios of comonomers, reaction conditions, and yields can be found in the Supporting Information.

Spin Coating. Thin films were prepared by spin coating with spin coater POLOS MCD200 (SPS-EUROPE B.V., The Netherlands). Heavily doped silicon wafers sputtered on both sides with aluminum (front side 50 nm, back side 300 nm) were used as substrates (1.5 × 2.0 cm^2). The solvents chosen were chloroform, methylene chloride (DCM), and ethyl methyl ketone (MEK) with a polymer concentration of 1−2 wt %. After spin coating at 2000 rpm for 30−60 s, the samples were dried under vacuum at 50 °C for 1 d.

Cross-linking. For photochemical cross-linking the samples were irradiated with UV light at the wavelengths of 254 and 366 nm for 2 h. In the case of thermal cross-linking of propargyl methacrylate (PgMA) copolymers, 1,3,5-tris(azidomethyl)benzene (TAMB) was added as cross-linker to the spin coating solution (33 mol % with respect to the content of PgMA in the copolymer to reach a molar ratio of R−N3 to R−C≡CH of 1/1 mol/mol). After spin coating, the samples were cross-linked under argon for 1 d at 130 °C (before drying). Additionally, the mixtures of PgMA containing copolymers and TAMB were also cross-linked photochemically (conditions see above). For cross-linking at room temperature using environmental humidity, 1,6-bis-(trichlorosilyl)hexane was added to the polymer solution (10 wt %

with respect to the polymer) and stored for 1 day in air, adapting a procedure reported in the literature.[1,13,19]

Self-supporting films were prepared to check cross-linking by deposition of polymer solutions on glass substrates. After solvent evaporation in air the films were removed and finally dried under vacuum. These films were cross-linked as mentioned above and their solubility was checked in chloroform.

Inkjet Printing. Inkjet printing of counter electrodes was carried out on a Dimatix Material Printer DMP-2800 (Fujifilm). PEDOT:PSS ink (CleviosTM P Jet 700 N, main component water, 10−25% ethanol, 5−10% diethylene glycol and less than 5% dimethyl sulfoxide) was obtained from Heraeus, silver neodecanoate (Ag Neo) was prepared according to Vest et al.[55] shortly before use and dissolved in xylene until saturated, silver nanoparticle (Ag NP) ink was a full finger line conductive ink obtained from XJET containing silver nanoparticles in a mixture of glycol ethers. Circular dots of different sizes (between 100 and 500 μm diameter, approximately) were printed on top of the dielectric layer. Printed PEDOT:PSS dots were dried at 50 °C under reduced pressure for 1 day or using a hot plate under nitrogen, Ag neo dots were annealed at 180 °C for 30 min and Ag NP dots were annealed at 130 °C for 30 min using a hot plate under nitrogen.

Device Characterization. Electrical characterizations were carried out with a SUSS PM6 Analytical Probe System (Karl Suss), Source Measurement Units K-2400 and K-6430 (Keithley) and an Agilent/HP 4294A Precision Impedance Analyzer (Hewlett-Packard). For the measurements of breakdown voltage and capacitance, metal−insulator−metal (MIM) structures were employed. The substrate was heavily doped silicon sputtered on the back side with 300 nm aluminum for back side contact (back side characterization). The front side was sputtered with 50 nm aluminum to form the MIM setup (aluminum−spin coated dielectric polymer−printed electrode dots). The breakdown voltage was defined as that voltage at which a current of 10 nA was detected. The capacitance was measured at a frequency of 1 MHz. Eq 3 was used to calculate the breakdown field strength, eq 4 were used to calculate the relative permittivity, where E_{BD} is the breakdown field strength, U_{BD} the breakdown voltage, d the film thickness (by ellipsometry), C the capacitance, ε_0 the permittivity of free space (8.854×10^{-12} As/Vm), k the relative permittivity of the dielectric layer, and A the area of the printed electrodes (by optical microscopy, Scandium).

$$E_{BD} = \frac{U_{BD}}{d} \tag{3}$$

$$C = \frac{\varepsilon_0 k A}{d} \tag{4}$$

■ ASSOCIATED CONTENT

Supporting Information

Synthesis, ^{1}H and ^{13}C NMR spectra of low molecular weight compounds; reaction conditions of radical polymerizations; ^{1}H NMR spectra of homo- and copolymers and determination of copolymer compositions; complete summary of all electrical characterizations (E_{BD}, k). This material is available free of charge via the Internet at http://pubs.acs.org.

■ AUTHOR INFORMATION

Corresponding Authors

*E-mail: berndt@ipfdd.de.
*E-mail: pospiech@ipfdd.de.

Notes

The authors declare no competing financial interest.

■ ACKNOWLEDGMENTS

This contribution is dedicated to Prof. Dr. rer. nat. habil. Manfred Stamm to the occasion of his 65th birthday. This study was financial supported by the Deutsche Forschungsgemeinschaft (DFG) and the German Excellence Initiative via the Cluster of Excellence EXC 1056 "Center for Advancing Electronics Dresden" (cfaed). We also thank Roland Schulze, Kerstin Arnhold and Petra Treppe from Leibniz-Institut für Polymerforschung Dresden e. V., and Michael Sawatski, Dr. Hans Kleemann and Dr. Simone Hoffmann from Institut für Angewandte Photophysik (TU Dresden). We thank Prof. Dr. Manfred Stamm for helpful discussions and support of the work. Prof. Dr. Mahmoud Al-Hussein thanks The University of Jordan and the Leibniz-Institut für Polymerforschung Dresden e. V. for financial support.

■ REFERENCES

(1) Yoon, M.-H.; Yan, H.; Facchetti, A.; Marks, T. J. Low-Voltage Organic Field-Effect Transistors and Inverters Enabled by Ultrathin Cross-Linked Polymers as Gate Dielectrics. *J. Am. Chem. Soc.* **2005**, *127*, 10388−10395.
(2) Howard, E. K.; Huang, J. Thin-Film Organic Electronic Devices. *Annu. Rev. Mater. Res.* **2009**, *39*, 71−92.
(3) Facchetti, A. π-Conjugated Polymers for Organic Electronics and Photovoltaic Cell Applications. *Chem. Mater.* **2011**, *23*, 733−758.
(4) Murphy, A. R.; Fréchet, J. M. J. Organic Semiconducting Oligomers for Use in Thin Film Transistors. *Chem. Rev.* **2007**, *107*, 1066−1096.
(5) Burroughes, J. H.; Bradley, D. D. C.; Brown, A. R.; Marks, R. N.; Mackay, K.; Friend, R. H.; Burns, P. L.; Holmes, A. B. Light-Emitting Diodes Based on Conjugated Polymers. *Nature* **1990**, *347*, 539−541.
(6) Sirringhaus, H.; Brown, P. J.; Friend, R. H.; Nielsen, M. M.; Bechgaard, K.; Langeveld-Voss, B. M. W.; Spiering, A. J. H.; Janssen, R. A. J.; Meijer, E. W.; Herwig, P.; de Leeuw, D. M. Two-Dimensional Charge Transport in Self-Organized, High-Mobility Conjugated Polymers. *Nature* **1999**, *401*, 685−688.
(7) Wen, Y. G.; Liu, Y. Q. Recent Progress in n-Channel Organic Thin-Film Transistors. *Adv. Mater.* **2010**, *22*, 1331−1345.
(8) Braga, D.; Horowitz, G. High-Performance Organic Field-Effect Transistors. *Adv. Mater.* **2009**, *21*, 1473−1486.
(9) Brabec, C. J.; Sariciftci, N. S.; Hummelen, J. C. Plastic Solar Cells. *Adv. Funct. Mater.* **2001**, *11*, 15−26.
(10) Mabeck, J. T.; Malliaras, G. G. Chemical and Biological Sensors Based on Organic Thin-Film Transistors. *Anal. Bioanal. Chem.* **2006**, *384*, 343−353.
(11) Samuel, I. D. W.; Turnbull, G. A. Organic Semiconductor Lasers. *Chem. Rev.* **2007**, *107*, 1272−1295.
(12) Crone, B.; Dodabalapur, A.; Lin, Y. Y.; Filas, R. W.; Bao, Z.; LaDuca, A.; Sarpeshkar, R.; Katz, H. E.; Li, W. Large-Scale Complementary Integrated Circuits Based on Organic Transistors. *Nature* **2000**, *403*, 521−523.
(13) Facchetti, A.; Yoon, M.-H.; Marks, T. J. Gate Dielectrics for Organic Field-Effect Transistors: New Opportunities for Organic Electronics. *Adv. Mater.* **2005**, *17*, 1705−1725.
(14) Peng, X.; Horowitz, G.; Fichou, D.; Garnier, F. All-Organic Thin-Film Transistors Made of Alpha-Sexithienyl Semiconducting and Various Polymeric Insulating Layers. *Appl. Phys. Lett.* **1990**, *57*, 2013−2015.
(15) Garnier, F.; Horowitz, G.; Peng, X.; Fichou, D. An All-Organic "Soft" Thin Film Transistor with Very High Carrier Mobility. *Adv. Mater.* **1990**, *2*, 592−594.
(16) Ortiz, R. P.; Facchetti, A.; Marks, T. J. High-k Organic, Inorganic, and Hybrid Dielectrics for Low-Voltage Organic Field-Effect Transistors. *Chem. Rev.* **2010**, *110*, 205−239.
(17) Veres, J.; Ogier, S.; Lloyd, G. Gate Insulators in Organic Field-Effect Transistors. *Chem. Mater.* **2004**, *16*, 4543−4555.
(18) Wilk, G. D.; Wallace, R. M.; Anthony, J. M. High-κ Gate Dielectrics: Current Status and Materials Properties Considerations. *J. Appl. Phys.* **2001**, *89*, 5243−5275.
(19) Noh, Y.-Y.; Sirringhaus, H. Ultra-Thin Polymer Gate Dielectrics for Top-Gate Polymer Field-Effect Transistors. *Org. Electron.* **2009**, *10*, 174−180.

(20) Park, J. H.; Hwang, D. K.; Lee, J.; Im, S.; Kim, E. Studies on Poly(methyl methacrylate) Dielectric Layer for Field Effect Transistor: Influence of Polymer Tacticity. *Thin Solid Films* **2007**, *515*, 4041−4044.
(21) Yu, H.-C.; Chen, Y.-C.; Huang, C.-Y.; Su, Y.-K. Investigation of Nonvolatile Memory Effect of Organic Thin-Film Transistors with Triple Dielectric Layers. *Appl. Phys. Express* **2012**, *5*, 034101−1−034101−3.
(22) Oh, J.-D.; Seo, H.-S.; Kim, D.-K.; Shin, E.-S.; Choi, J.-H. Device Characteristics of Perylene-Based Transistors and Inverters Prepared with Hydroxyl-Free Polymer-Modified Gate Dielectrics and Thermal Post-Treatment. *Org. Electron.* **2012**, *13*, 2192−2200.
(23) Lavina, S.; Negro, E.; Pace, G.; GHross, S.; Depaoli, G.; Vidali, M.; Di Noto, V. Dielectric Low-k Composite Films Based on PMMA, PVC and Methylsiloxane-Silica: Synthesis, Characterization and Electrical Properties. *J. Non-Cryst. Solids* **2007**, *353*, 2878−2888.
(24) Baeg, K.-J.; Khim, D.; Jung, S.-W.; Kang, M.; You, I.-K.; Kim, D.-Y.; Facchetti, A.; Noh, Y.-Y. Remarkable Enhancement of Hole Transport in Top-Gated N-Type Polymer Field-Effect Transistors by a High-k Dielectric for Ambipolar Electronic Circuits. *Adv. Mater.* **2012**, *24*, 5433−5439.
(25) Yan, H.; Chen, Z.; Zheng, Y.; Newman, C.; Quinn, J. R.; Dötz, F.; Kastler, M.; Facchetti, A. A High-Mobility Electron-Transporting Polymer for Printed Transistors. *Nature* **2009**, *457*, 679−687.
(26) Cheng, J.-A.; Chuang, C.-S.; Chang, M.-N.; Tsai, Y.-C.; Shieh, H.-P. D. Controllable Carrier Density of Pentacene Field-Effect Transistors Using Polyacrylates as Gate Dielectrics. *Org. Electron.* **2008**, *9*, 1069−1075.
(27) Halik, M.; Klauk, H.; Zschieschang, U.; Kriem, T.; Schmid, G.; Radlik, W.; Wussow, K. Fully Patterned All-Organic Thin Film Transistors. *Appl. Phys. Lett.* **2002**, *81*, 289−291.
(28) Parashokov, R.; Becker, E.; Ginev, G.; Riedl, T.; Johannes, H.-H.; Kowalsky, W. All-Organic Thin-Film Transistors Made of Poly(3-butylthiophene) Semiconducting and Various Polymeric Insulating Layers. *J. Appl. Phys.* **2004**, *95*, 1594−1569.
(29) Virkar, A. A.; Mannsfeld, S.; Bao, Z.; Stingelin, N. Organic Semiconductor Growth and Morphology Considerations for Organic Thin-Film Transistors. *Adv. Mater.* **2010**, *22*, 3857−3875.
(30) Lee, H. S.; Kim, D. H.; Cho, J. H.; Hwang, M.; Jang, Y.; Cho, K. A. Effect of the Phase States of Self-Assembled Monolayers on Pentacene Growth and Thin-Film Transistor Characteristics. *J. Am. Chem. Soc.* **2008**, *130*, 10556−10564.
(31) Lin, Y. Y.; Gundlach, D. J.; Nelson, S. F.; Jackson, T. N. Stacked Pentacene Layer Organic Thin-Film Transistors with Improved Characteristics. *IEEE Electron Device Lett.* **1997**, *18*, 606−608.
(32) Tang, M. L.; Roberts, M.; Locklin, J.; Ling, M.; Meng, H.; Bao, Z. Structure Property Relationships: Asymmetric Oligofluorene-Thiophene Molecules for Organic TFTs. *Chem. Mater.* **2006**, *18*, 6250−6257.
(33) Ito, Y.; Virkar, A. A.; Mannsfeld, S. C. B.; Oh, J. H.; Toney, M. F.; Locklin, J.; Bao, Z. Crystalline Ultrasmooth Self-Assembled Monolayers of Alkylsilanes for Organic Field-Effect Transistors. *J. Am. Chem. Soc.* **2009**, *131*, 9396−9404.
(34) Pospiech, D.; Jehnichen, D. In *Handbook of Fluoropolymer Science & Technology*; Smith, D. W., Iacono, S. T., Iyer, S. S., Eds.; John Wiley & Sons: Hoboken, NJ, 2014; Chapter 11, pp 235−290.
(35) Craig, A. A.; Imrie, C. T. Effect of Spacer Length on the Thermal Properties of Side-Chain Liquid Crystal Polymethacrylates. 2. Synthesis and Characterization of the Poly[.omega.-(4′-cyanobiphenyl-4-yloxy)-alkyl methacrylate]s. *Macromolecules* **1995**, *28*, 3617−3624.
(36) Zhang, Y.; He, H.; Gao, C.; Wu, J. Covalent Layer-by-Layer Functionalization of Multiwalled Carbon Nanotubes by Click Chemistry. *Langmuir* **2009**, *25*, 5814−5824.
(37) Piskunov, M. V.; Kostromin, S. G.; Stroganov, L. B.; Shibaev, V. P.; Platé, N. A. Thermotropic Liquid Crystalline Polymers, 9. Proton Magnetic Resonance Study of Orientation of Liquid-Crystalline Comb-Shaped Polymers in a Magnetic Field. *Makromol. Chem. - Rapid* **1982**, *3*, 443−447.
(38) Kostromin, S. G.; Sinitsyn, V. V.; Tal'roze, R. V.; Shibayev, V. P. Structure of Thermotropic Liquid Crystalline Polymers with Cyano-Containing Mesogenic Groups. *Polym. Sci. U.S.S.R.* **1984**, *26*, 370−382.
(39) Shibayev, V. P.; Kostromin, S. G.; Platé, N. A. Thermotropic Liquid-Crystalline Polymers—VI: Comb-Like Liquid-Crystalline Polymers of the Smectic and Nematic Types with Cyanobiphenyl Groups in the Side-Chains. *Eur. Polym. J.* **1982**, *18*, 651−659.
(40) Yamada, M.; Itoh, T.; Nakagawa, R.; Hirao, A.; Nakahama, S.; Watanabe, J. Synthesis of Side-Chain Liquid Crystalline Homopolymers and Block Copolymers with Cyanobiphenyl Moieties as the Mesogen by Living Anionic Polymerization and Their Thermotropic Phase Behavior. *Macromolecules* **1999**, *32*, 282−289.
(41) Al-Hussein, M.; de Jeu, W. H.; Vranichar, L.; Pispas, S.; Hadjichristidis, N.; Itoh, T.; Watanabe, J. Bulk and Thin Film Ordering in Side-Chain Liquid-Crystalline/Amorphous Diblock Copolymers: The Role of Chain Length. *Macromolecules* **2004**, *37*, 6401−6407.
(42) Gratacòs, N. Q. *Functional Hydrogels: Ferrogel Thin Films*. Ph.D. Thesis, Johanees Gutenberg-Universität, Mainz, Germany, 2010.
(43) Dormán, G.; Prestwich, G. D. Benzophenone Photophores in Biochemistry. *Biochemistry* **1994**, *33*, 5661−5673.
(44) Huisgen, R. 1,3-Dipolar Cycloadditions. Past and Future. *Angew. Chem., Int. Ed.* **1963**, *2*, 565−632.
(45) Bräse, S.; Gil, C.; Knepper, K.; Zimmermann, V. Organic Azides: An Exploding Diversity of a Unique Class of Compounds. *Angew. Chem., Int. Ed.* **2005**, *44*, 5188−5240.
(46) Hoesch, L. Nitrene - Bausteine einer organischen Stickstoffchemie. *Chem. unserer Zeit* **1976**, *10*, 54−61.
(47) Al Akhrass, S.; Damiron, D.; Carrot, G.; Drockenmuller, E. Photo-Crosslinked Fluorinated Thin Films from Azido-Functionalized Random Copolymers. *J. Polym. Sci., Part A: Polym. Chem.* **2010**, *48*, 3888−3895.
(48) Hafner, K.; Zinser, D.; Moritz, K. L. Reaktionen von Benzolderivaten mit Nitrenen. *Tetrahedron Lett.* **1964**, *26*, 1733−1737.
(49) Bang, J.; Bae, J.; Löwenhielm, P.; Spiessberger, C.; Given-Beck, S. A.; Russell, T. P.; Hawker, C. J. Facile Routes to Patterned Surface Neutralization Layers for Block Copolymer Lithography. *Adv. Mater.* **2007**, *19*, 4552−4557.
(50) Xu, W.; Rhee, S.-W. Hysteresis-Free Organic Field-Effect Transistors with High Dielectric Strength Cross-Linked Polyacrylate Copolymer as a Gate Insulator. *Org. Electron.* **2010**, *11*, 836−845.
(51) Pielichowski, K.; Njuguna, J. *Thermal Degradation of Polymeric Materials*; Rapra Technology: Shropshire, U.K., 2005.
(52) Brandrup, J.; Immergut, E. H.; Grulke, E. A. *Polymer Handbook*, 4th ed.; John Wiley & Sons.: Hoboken, NJ, 1999.
(53) Kim, S. H.; Yang, S. Y.; Shin, K.; Jeon, H.; Lee, J. W.; Hong, K. P.; Park, C. E. Low-Operating-Voltage Pentacene Field-Effect Transistor with a High-Dielectric-Constant Polymeric Gate Dielectric. *Appl. Phys. Lett.* **2006**, *89*, 183516−183518.
(54) Cobet, C. In *Ellipsometry of Functional Organic Surfaces and Films*; Hinrichs, K., Eichhorn, K.-J., Eds.; Springer-Verlag: Berlin Heidelberg, 2014; Chapter 1, pp 1−28.
(55) Vest, G. M.; Singaram, S. Synthesis of Metallo-Organic Compounds for Mod Powders and Films. *MRS Online Proc. Libr.* **1985**, *60*, 35−42.